

ornl

**OAK RIDGE
NATIONAL
LABORATORY**

MARTIN MARIETTA

OPERATED BY
MARTIN MARIETTA ENERGY SYSTEMS, INC.
FOR THE UNITED STATES
DEPARTMENT OF ENERGY



3 4456 0064925 2

ORNL/TM-9906

Feasibility Study of a Cryogenically Cooled Window for High-Power Gyrotrons

G. R. Haste
H. D. Kimrey
J. D. Prorise

OAK RIDGE NATIONAL LABORATORY

CENTRAL RESEARCH LIBRARY

CIRCULATION SECTION

ROOM 2009 L15

LIBRARY LOAN COPY

DO NOT TRANSFER TO ANOTHER PERSON

If you wish someone else to see this
report, send in name with report and
the library will arrange a loan.

10/24/78

Printed in the United States of America. Available from
National Technical Information Service
U.S. Department of Commerce
5285 Port Royal Road, Springfield, Virginia 22161
NTIS price codes—Printed Copy: A03; Microfiche A01

This report was prepared as an account of work sponsored by an agency of the United States Government. Neither the United States Government nor any agency thereof, nor any of their employees, makes any warranty, express or implied, or assumes any legal liability or responsibility for the accuracy, completeness, or usefulness of any information, apparatus, product, or process disclosed, or represents that its use would not infringe privately owned rights. Reference herein to any specific commercial product, process, or service by trade name, trademark, manufacturer, or otherwise, does not necessarily constitute or imply its endorsement, recommendation, or favoring by the United States Government or any agency thereof. The views and opinions of authors expressed herein do not necessarily state or reflect those of the United States Government or any agency thereof.

ORNL/TM-9906
Dist. Category UC-20

Fusion Energy Division

**FEASIBILITY STUDY OF A CRYOGENICALLY COOLED WINDOW
FOR HIGH-POWER GYROTRONS**

G. R. Haste
H. D. Kimrey
J. D. Prorise*

*Martin Marietta Energy Systems, Inc., Engineering Division.

Date of Issue: July 1986

Prepared by the
OAK RIDGE NATIONAL LABORATORY
Oak Ridge, Tennessee 37831
operated by
MARTIN MARIETTA ENERGY SYSTEMS, INC.
for the
U.S. DEPARTMENT OF ENERGY
under Contract No. DE-AC05-84OR21400



3 4456 0064925 2

CONTENTS

ABSTRACT	1
1. INTRODUCTION	1
2. MODEL	1
2.1 PRESENT WINDOW STATUS	1
2.2 ANALYSIS TECHNIQUES	3
3. ADVANTAGES OF OPERATION AT CRYOGENIC TEMPERATURES	5
3.1 DIELECTRIC HEATING	5
3.2 THERMAL CONDUCTIVITY	6
3.3 THERMAL EXPANSION	7
3.4 YOUNG'S MODULUS	7
3.5 SLOW CRACK GROWTH	8
3.6 COOLING FLUID	8
4. TEMPERATURE DISTRIBUTIONS AT CRYOGENIC TEMPERATURES ...	9
4.1 HELIUM-COOLED DOUBLE DISK WINDOW	9
4.2 LIQUID NITROGEN—COOLED DOUBLE DISK WINDOW	10
4.3 EDGE-COOLED WINDOW	12
4.4 OTHER HEAT LOADS	16
4.4.1 Conduction	16
4.4.2 Radiation	16
5. CONCLUSIONS	16
REFERENCES	19

A FEASIBILITY STUDY OF A CRYOGENICALLY COOLED WINDOW FOR HIGH-POWER GYROTRONS

G. R. Haste, H. D. Kimrey, and J. D. Prosis

ABSTRACT

Single-crystal sapphire is currently in use as the material for output windows in high-power microwave tubes, particularly gyrotrons. These windows are currently being cooled by fluorocarbon fluids at near-room temperatures. There are, however, several advantages in operating the window at very low temperatures: less absorption and consequent heating of the window, greater material strength, improved resistance to crack formation, greater thermal conductivity, and reduced thermal expansion. Operation at cryogenic temperatures is shown to be feasible. The output power, which is currently limited by window constraints, could be increased by an order of magnitude or more.

1. INTRODUCTION

The output window of a microwave tube has as its principal function to separate the high vacuum in the tube interior from the exterior atmosphere. In doing so, it must transmit the microwave power generated by the tube with little attenuation. More precisely, there must be very little absorption in the window because the heat deposited has to be removed. The temperature rise associated with the heat deposition results in thermal stress—stress that can be high enough to break the window.

The experience with gyrotrons to date has demonstrated that the most likely cause of tube failure is window fracture. An improved window offers the prospect of enhanced reliability in tube operation. Many of the material characteristics are improved at low temperatures, so a feasibility study of a cooled window seems warranted.

The conclusion of this study is that such a cooled window is in fact feasible, with no state-of-the-art improvements necessary. The principal difficulty is in removing the heat generated in the window, just as it is for windows operating near ambient temperatures. Our conclusion is that a 1-MW cw window at 140 GHz can be achieved with present-day technology and that a 10-MW window may be possible.

2. MODEL

2.1 PRESENT WINDOW STATUS

Some of the earlier gyrotrons used output windows that consisted of a single ceramic disk operating at room temperature and cooled only at the edge. When the single disk

design was shown to be inadequate (due to thermal stress), it was replaced with a double disk design, in which a dielectric fluid flowed between the two disks to remove the heat. The fluid in most common use is a fluorocarbon ("freon") known as FC-75. Both of these designs (single and double disk, or alternatively edge cooled and face cooled) will be considered in this feasibility study. These two designs are shown schematically in Figs. 1 and 2. To date, the highest cw power transmitted has been 120 kW and 340 kW at 28 GHz for the single and double disk windows respectively. The double disk window has also transmitted 200 kW at 60 GHz.

Many of the present gyrotrons use alumina windows, which are composed of polycrystalline aluminum oxide. Recently, it has been decided to use sapphire, which is single-crystal aluminum oxide, on newer gyrotrons. The reasons are that, although the alumina is a tougher material than sapphire and can therefore withstand stress better, it also has a higher microwave absorptivity. More heat is produced in an alumina window than in a sapphire window, so more thermal stress is generated, and the operating margin is lower for alumina. It has been projected that, at room temperature, sapphire double disk windows will be able to transmit 100 to 200 kW of power at 140 GHz, whereas alumina will transmit only 50 to 60 kW of power.

ORNL-DWG 85-3688 FED

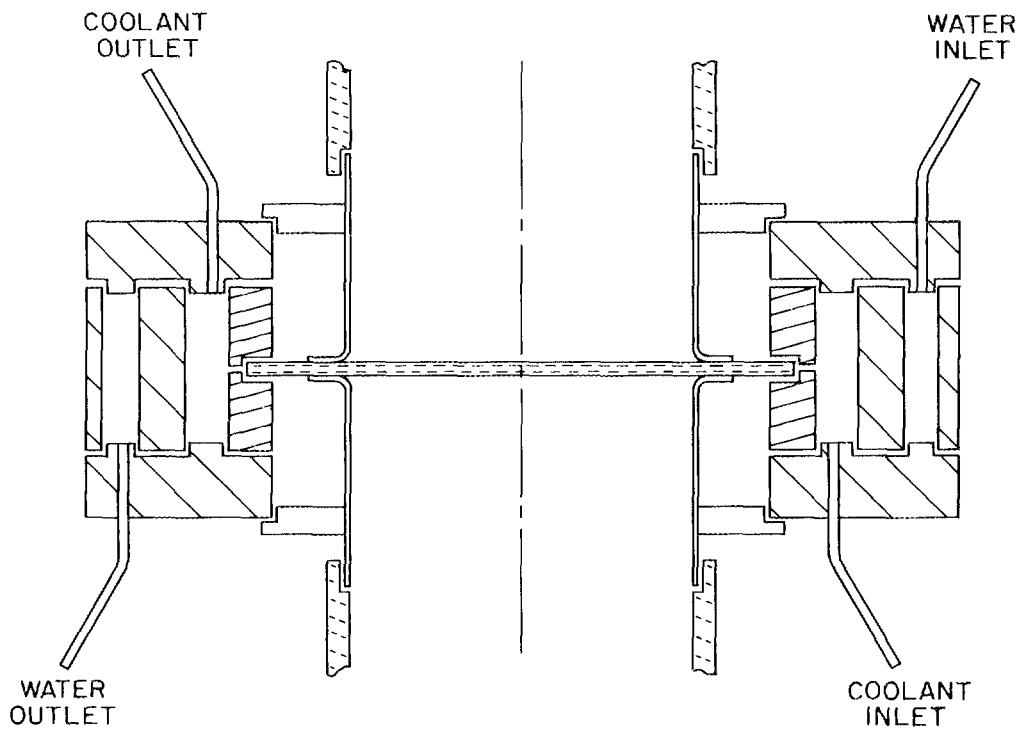


Fig. 1. Schematic of single disk output window for microwave tube.

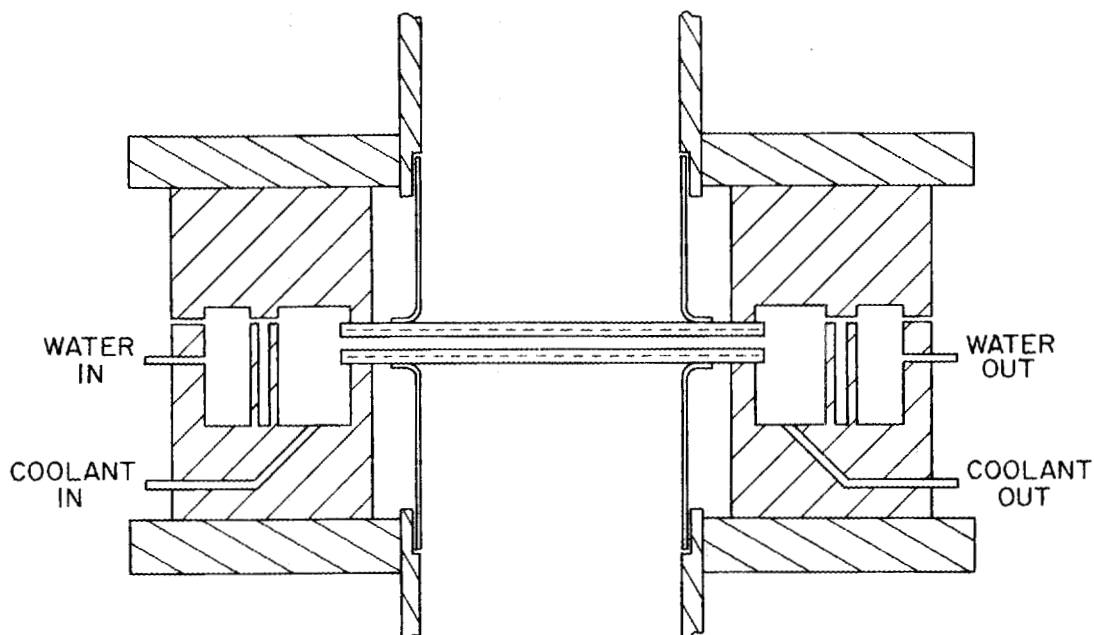


Fig. 2. Schematic of double disk output window for microwave tube.

The microwave loss in sapphire is one of the lowest for candidate materials for gyrotron windows. This is demonstrated in Fig. 3, which shows the loss tangent¹ ($\tan \delta$ is the ratio of the imaginary to the real part of the dielectric constant) for several window materials as a function of frequency. This figure also shows that although the loss is lowest in sapphire, it increases with frequency. As a result, a window that is acceptable at lower frequency can be intolerable at higher frequency.

2.2 ANALYSIS TECHNIQUES

The stress is analyzed² by determining the temperature distribution, using the heat conduction equation

$$\nabla^2 T + \frac{q'''}{k_t} = \frac{1}{D_t} \frac{\partial T}{\partial t}, \quad (1)$$

where D_t is the thermal diffusivity, k_t is the thermal conductivity, and q''' is the thermal power density due to dielectric heating.

The thermal power density can be written as

$$q''' = \left(\frac{\omega}{2} \epsilon_r \epsilon_0 \tan \delta \right) |E_p|^2, \quad (2)$$

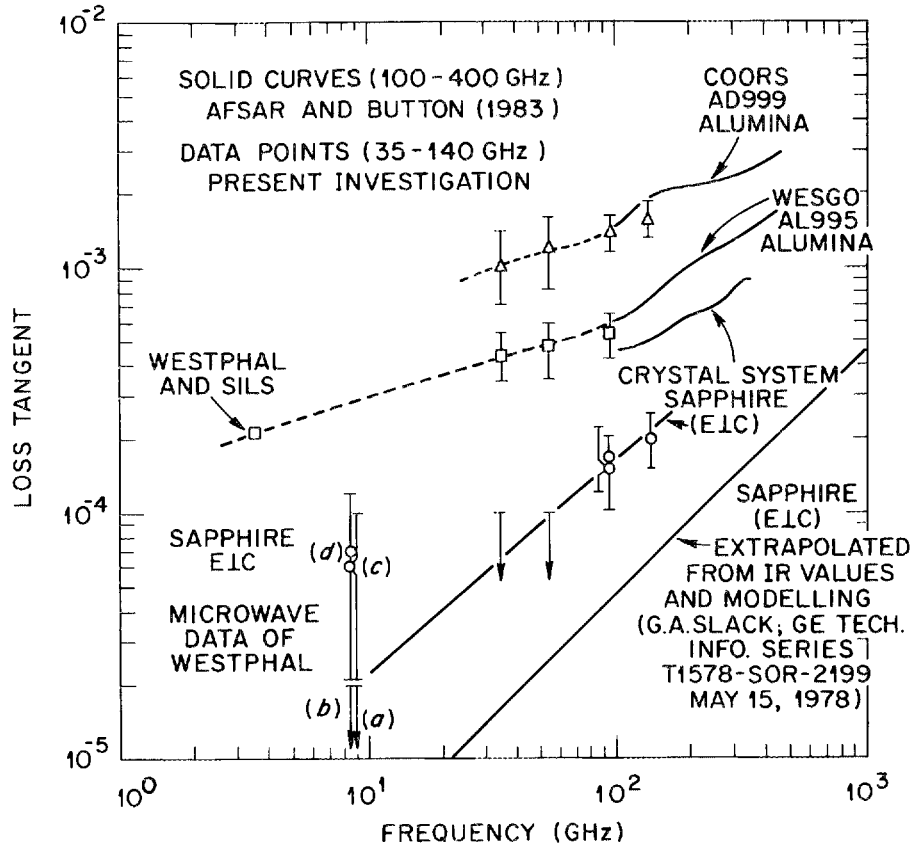


Fig. 3. Variation of loss tangent with microwave frequency for various materials.

where ω is the (radian) frequency, ϵ_r is the relative dielectric constant, ϵ_0 is the permittivity of free space, $\tan \delta$ is the loss tangent, defined above, and $|E_p|$ is the magnitude of the peak electric field, which is spatially varying and is determined by the waveguide mode.

The radial and tangential stresses (σ_r and σ_t) can be determined from the temperature distribution:

$$\sigma_r = (\alpha Y) \left[\frac{I}{R_0^2} - \left(\frac{1}{r^2} \right) \int_0^r T(r) r dr \right], \quad (3a)$$

$$\sigma_t = (\alpha Y) \left[\frac{I}{R_0^2} + \left(\frac{1}{r^2} \right) \int_0^r T(r) r dr - T(r) \right], \quad (3b)$$

$$I = \int_0^{R_0} T(r) r dr. \quad (3c)$$

In these equations, R_0 is the window radius, α is the thermal expansion coefficient, and Y is the Young's modulus.

3. ADVANTAGES OF OPERATION AT CRYOGENIC TEMPERATURES

Many of the parameters that enter in determining the window stress are much improved at low temperature. As a result, *if the window temperature can be kept low*, very large reductions in the stress level will occur. In fact, at cryogenic temperatures thermal stress is no longer (directly) the limiting mechanism. Output power is limited instead by thermal runaway. The temperature variation of these parameters is discussed below.

3.1 DIELECTRIC HEATING

Dielectric heating of the sapphire appears to be the most crucial aspect of the cryogenic window. Although the available data on the dielectric properties of sapphire at reduced temperatures are scant, we present here a scaling model for frequency and temperature variations based on the available data. Although this scaling model projects favorably for cryogenic operation, we emphasize that a detailed investigation of sapphire should be performed in the millimeter wavelength range, rather than relying on model projections.

Several excellent experimental studies^{3,4} of sapphire in the far infrared have shown the temperature dependence on the absorption coefficient to be roughly $T^{2.5}$. Unfortunately, these high-frequency measurements did not extend down into the millimeter wave region. At the low-frequency end of the spectrum, using high- Q superconducting cavities, the loss tangent of sapphire has been determined to be 2×10^{-9} at 2.9 GHz and 4.2 K.⁵ We use this number together with Ho's results¹ (Fig. 3) at room temperature to obtain our model.

If it is assumed that the frequency and temperature variations of loss tangent are uncoupled, then a trial fitting function is

$$\tan \delta = C f^x T^y . \quad (4)$$

Fits to the data yield $C = 5.58 \times 10^{-11}$, $x = 0.717$, and $y = 1.96$ where f is in gigahertz and T is in degrees Kelvin. This model is consistent with a recent measurement¹ of sapphire at 100 GHz and 80 K, in which the measured loss tangent was below the sensitivity of the apparatus, or 5×10^{-5} . Equation 4 yields 8.1×10^{-6} , which is an encouraging consistency.

Once the loss tangent is known, the losses for the window can be calculated. A simple relation can be derived for the absorption coefficient for a window whose thickness is n half-wavelengths:

$$A = \frac{n\pi}{2} \tan \delta \left[\sqrt{\epsilon_r} + \frac{1}{\sqrt{\epsilon_r}} \right] . \quad (5)$$

Combining equations (4) and (5) yields

$$A = 8.77 \times 10^{-11} n f^{0.717} T^{1.96} \left(\sqrt{\epsilon_r} + \frac{1}{\sqrt{\epsilon_r}} \right) \text{ W/MW} . \quad (6)$$

Equation (6) will be used to evaluate the potential power throughput of the cryogenic window.

3.2 THERMAL CONDUCTIVITY

As can be seen from Eq. (1), the driving term in the heat conduction equation is the thermal power density divided by the thermal conductivity. As discussed above, indications are that the thermal power density will be reduced at low temperatures. In contrast to the minimal data to support that point, there are excellent data concerning the temperature variation of the thermal conductivity. This variation is shown in Fig. 4 for sapphire.⁶ To illustrate a point, the thermal conductivities of copper and diamond are shown in the same figure. A comparison between sapphire at room temperature (~ 300 K) and liquid nitrogen temperature (~ 80 K) shows a factor of 20 increase in conductivity for sapphire. Thus, if the corresponding absorptive losses were reduced by a factor of 4, then there would be a factor of 80 reduction in the driving term.

Some appreciation for the magnitude of the thermal conductivity can be gained by noting that, at 80 K, the sapphire conductivity is better than that for copper. It is, however, not as good as that for diamond.

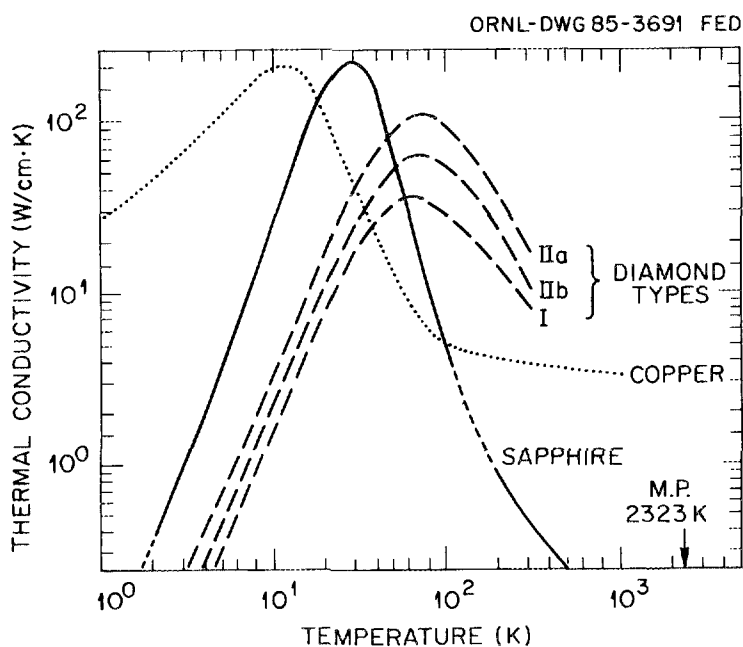


Fig. 4. Thermal conductivity as a function of temperature for various materials.

While the large conductivity value is encouraging, the rapid variation with temperature is a cause for concern. A potentially unstable situation can arise as follows: as the temperature increases at a certain location, the conductivity decreases so the heat tends to remain where generated, thereby raising the temperature further, etc. This process manifests itself in some of the calculations that follow in that below some critical power level the temperature is quite reasonable, but above that level the temperature rapidly rises. This is referred to as thermal runaway.

Figure 4 also illustrates the attractiveness of operation at 20–30 K. Not only is the conductivity much higher there, but the temperature variation is small, so runaway would be expected only at much greater powers.

3.3 THERMAL EXPANSION

The relation between the thermal stress and the temperature distribution, given in Eq. (3), shows that the stress is proportional to the thermal expansion coefficient. The temperature variation of that parameter is also favorable,⁷ as shown in Table 1. As this table shows, thermal expansion becomes very low at low temperatures. As a result, a given temperature distribution leads to much smaller stresses.

3.4 YOUNG'S MODULUS

The proportionality between the temperature distribution and the stress depends not only on the thermal expansion coefficient but on the Young's modulus as well. The temperature variation of this parameter is in the unfavorable direction: the material becomes stiffer at low temperature and the Young's modulus increases. However, this effect is

Table 1. Thermal expansion for sapphire

Temperature (K)	α	
	$\parallel c$ axis	$\perp c$ axis
23	0.0	0.0
48	0.0	0.0
73	0.2	0.1
123	1.2	0.9
173	2.6	2.2
223	4.0	3.5
273	5.2	4.6
293	5.6	5.0
373	6.8	6.2

extremely small,⁸ as shown in Fig. 5. The variation between 300 and 0 K is only 0.7%. At that level it may be assumed to be independent of temperature.

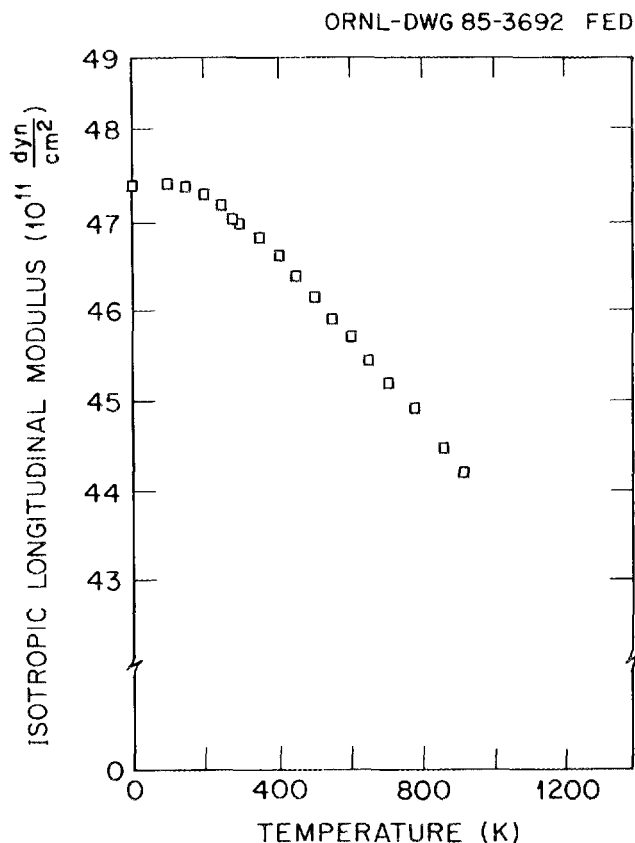


Fig. 5. Temperature variation of longitudinal modulus for single-crystal sapphire.

3.5 SLOW CRACK GROWTH

It has been demonstrated⁹ that windows rarely fail from a catastrophic fracture but from the growth of small cracks under the influence of the applied stress. Water helps promote slow crack growth, both as vapor in the air and as a small impurity in fluorocarbon fluids. However, the chemical activity of water drops to essentially zero at liquid nitrogen temperatures. As a result, a sample that would fail at a given stress level in a few minutes at room temperature will last indefinitely at 77 K. In turn, at low temperatures, the tolerable stress level can approach the fracture strength of the material.

3.6 COOLING FLUID

The use of fluorocarbons as the cooling medium is a concern. In the event of a window failure, the cooling fluid could encounter hot surfaces and decompose into hazardous

products. With a cryogenically cooled window, these concerns are alleviated because the fluids are likely to be nitrogen or helium, which are inert.

4. TEMPERATURE DISTRIBUTIONS AT CRYOGENIC TEMPERATURES

The previous discussion has shown that a number of benefits can be expected from low-temperature operation. However, to obtain these benefits, the window must be kept cold, and that requires removal of the heat produced. Unfortunately, no large factors can be gained in heat transfer, so this area is clearly the most critical issue. As shown below, this problem appears solvable with standard techniques.

The calculations assume that heat is uniformly generated within the central 2.5-cm diameter of a 10-cm-diam sapphire disk. This is an attempt to model the actual heat deposition profile, which depends on the distribution of the microwave electric fields. Since the most intense heating occurs at the first radial maximum, the uniform heating in the center is a reasonable approximation. This model is conservative, however, in that all of the power is deposited near the center, as opposed to being distributed throughout the window.

As mentioned previously, both face-cooled and edge-cooled windows will be considered for various coolant fluids. Since the central issue affecting the feasibility of a cryogenically cooled window is the ability to remove the heat, most of the work has involved determining heat transfer characteristics. The double disk window is examined first as it has transmitted the highest average power thus far. The resulting radial temperature distributions are presented in the following paragraphs.

4.1 HELIUM-COOLED DOUBLE DISK WINDOW

The simplest cooling scheme would be simply to flow liquid nitrogen between the disks. The trouble with that approach is that the liquid is very likely to boil within the window. A pure waveguide mode, incident on such a two-phase, inhomogeneous medium, would be converted to a mix of modes, which is detrimental to waveguide attenuation and launching. Consequently, operation with a single-phase coolant is necessary. The simplest system that guarantees single-phase cooling would be a gaseous helium system that utilizes a liquid nitrogen heat exchanger.

Two cases involving gaseous helium coolant were analyzed: one with a helium temperature of 80 K, which is achievable by means of a liquid nitrogen heat exchanger, and one with a fluid temperature of 30 K, which would require the addition of a helium refrigerator to the system. An in-house heat transfer code (Heating-6) was used in the analysis. The most critical phase in building the model was in determining proper values for the film coefficients to quantify the heat transfer potential between the face of the window and the cooling medium. Flow between the double disks was modeled as duct flow using the hydraulic diameter of the flow passage, and the convection coefficient was allowed to vary with average film temperature. Calculations were based on an assumed helium mass flow rate of 10 g/s.

As Fig. 6 shows, heat removal with helium at a nominal temperature of 80 K would be adequate for an absorption of 100 W, resulting in a radial temperature gradient of

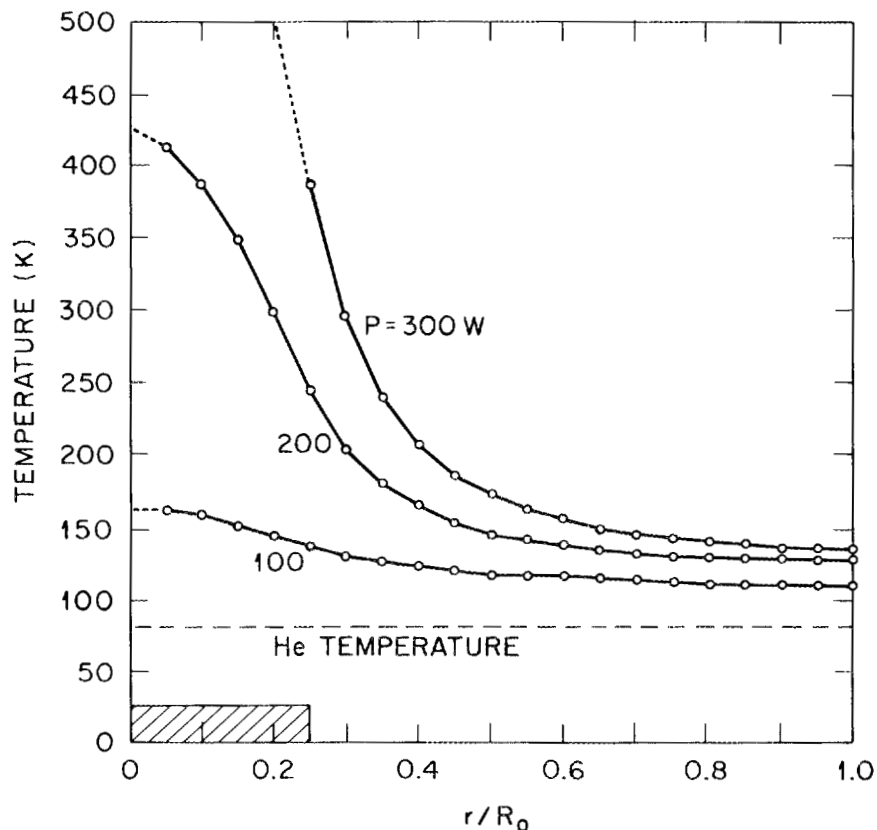


Fig. 6. Temperature distributions in one disk of a double disk window for various amounts of power deposited in the center of the disk. The coolant is gaseous helium at 80 K.

approximately 30 K. The average temperature is ~ 140 K. This power absorption, according to Eq. (6), would be achieved for 100 kW at 140 GHz, for $n = 4$ and $\epsilon_r = 9.4$. Cooling would be insufficient at higher powers. Figure 7 shows the improvement in the thermal profile of the window for a helium temperature of 30 K. As mentioned in the section on thermal conductivity, operating at the temperature where the thermal conductivity is a maximum appears to have some advantages. The tolerable heat removal level would rise to about 400 W, corresponding to an output power level of 800 kW.

4.2 LIQUID NITROGEN-COOLED DOUBLE DISK WINDOW

The principal difficulty with using liquid nitrogen as a coolant is the possibility of boiling, or phase transition, within the window. This possibility is more accurately termed a likelihood due to the highly localized heat load inside the window. This difficulty might be alleviated if (1) the bubbles formed in the boiling process might be so few or so small in size that they would not affect microwave transmission or mode conversion, or (2) the

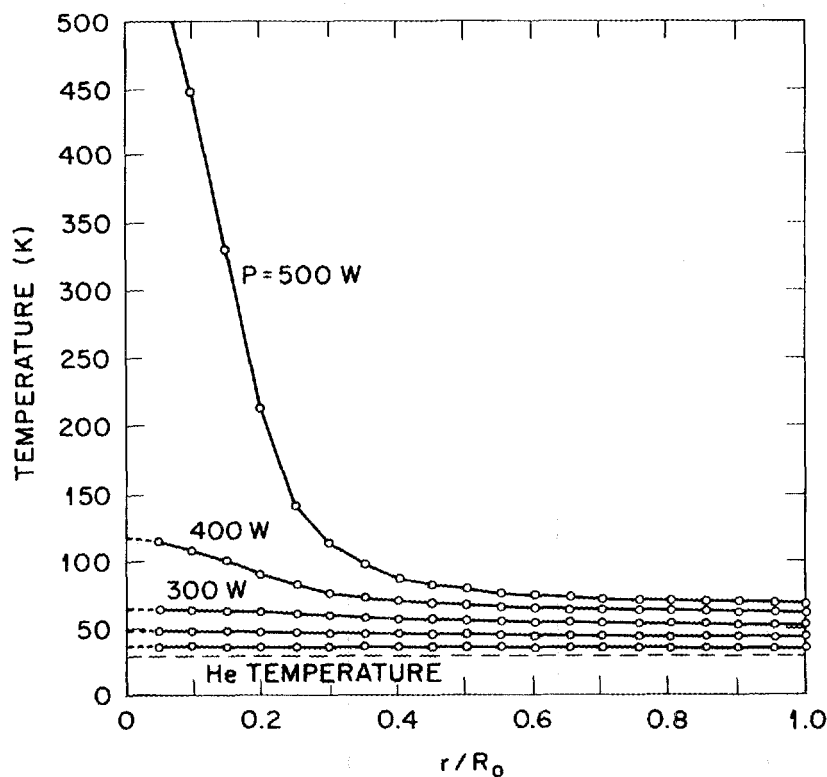


Fig. 7. Temperature distributions in one disk of a double disk window for various amounts of power deposited in the center of the disk. The coolant is gaseous helium at 30 K.

liquid nitrogen could be subcooled or compressed to some degree, moving it away from near-saturated liquid conditions, by lowering its temperature, pressurizing it, or some combination of both.

If the two-phase problem could be solved, then cooling with liquid nitrogen would be very attractive. With a flow rate of 10 gal/min, a heat transfer coefficient of $1.5 \text{ W}/(\text{cm}^2 \cdot \text{K})$ could be expected, representing an improvement in heat removal ability over helium of better than an order of magnitude. That value for the film coefficient would result in the temperature distribution shown in Fig. 8. The same figure, however, illustrates why two-phase flow is likely. At a 500-W absorption level, the window reaches a maximum surface temperature of about 125 K. Preventing vapor formation in liquid nitrogen at 100 K requires pressurization to a minimum of $\sim 8 \text{ atm}$, a measure not available because it would induce stresses in the disk on the order of $1 \times 10^5 \text{ psi}$ in addition to the thermal stresses. Subcooling the nitrogen to 67 K initially would offer some degree of relief; however, doing so would require the use of a refrigerator unit, a requirement that would add to the cost and complexity of the cooling system and still could not ensure single-phase flow. In fact, any effort to predict the chances of a phase transition is further

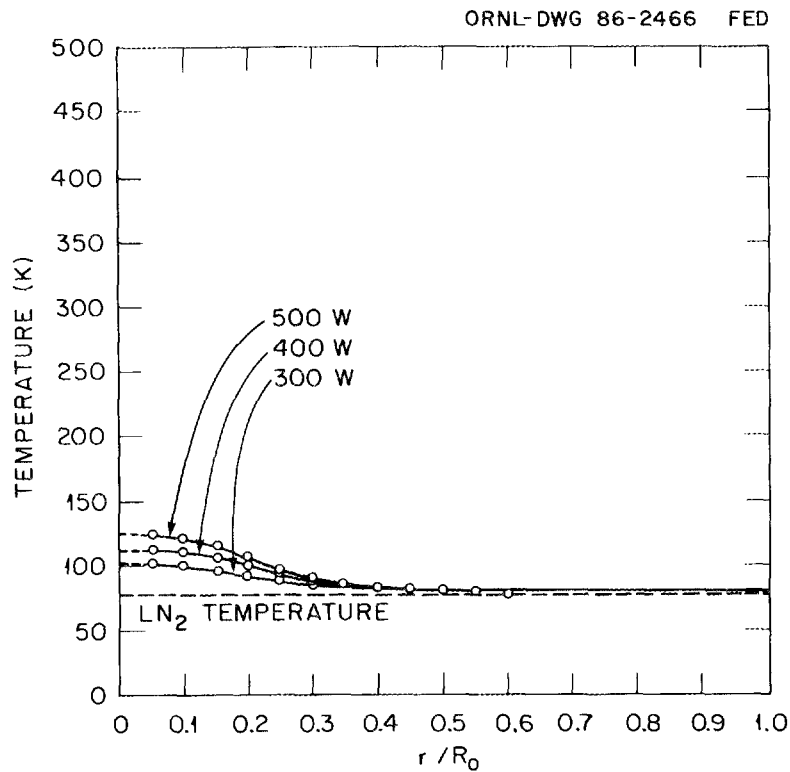
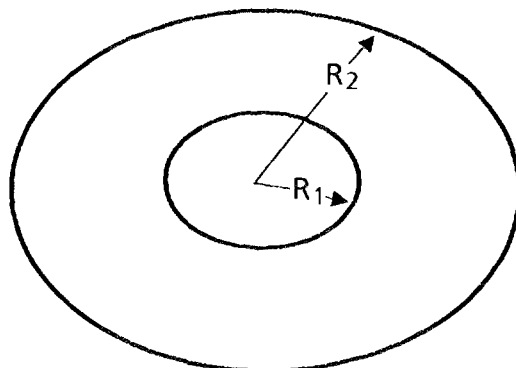


Fig. 8. Temperature distributions in one disk of a double disk window for various amounts of power deposited in the center of the window. The coolant is liquid nitrogen at 80 K.

hampered by other factors such as heat leakage through the pipes (both through the insulation and down the walls of the pipe) and pressure drops induced by piping components, such as valves.

4.3 EDGE-COOLED WINDOW

For the case with the heat deposition at the center of the window and the heat removal at the edge, the heat flow is purely radial and the problem is sufficiently simple that analytic techniques can be used to determine the temperature distribution.



The sketch above can be used to define the geometry: an amount of heat P_T is uniformly deposited within the central disk of radius R_1 , the heat is removed at R_2 . In steady state the heat flux across a cylindrical surface will equal the heat generated within that surface. If the thickness of the disk is a , then the heat flux will be

$$\Phi(r) = \frac{P_T r}{2\pi R_1^2 a} \quad \text{for } r < R_1, \quad (7a)$$

and

$$\Phi(r) = \frac{P_T}{2\pi r a} \quad \text{for } R_1 < r < R_2. \quad (7b)$$

Since the heat flux is also related to the thermal gradient,

$$\Phi(r) = -k_t \frac{dT}{dr}. \quad (8)$$

By equating the heat flux from Eqs. (7) and (8), a differential equation for the temperature is obtained. If k_t is chosen to be independent of radius, then the solutions are

$$T(r) = T_{\text{edge}} + \frac{P_T}{2\pi k_t a} \ln \frac{R_2}{R_1} + \frac{0.5P_T}{2\pi k_t a} \left[1 - \left(\frac{r}{R_1} \right)^2 \right] \quad \text{for } r < R_1, \quad (9a)$$

and

$$T(r) = T_{\text{edge}} + \frac{P_T}{2\pi k_t a} \ln \frac{R_2}{r} \quad \text{for } R_1 < r < R_2. \quad (9b)$$

The edge temperature differs from the coolant temperature by the film drop.

$$T_{\text{edge}} = T_{\text{coolant}} + \frac{P_T}{hA}. \quad (10)$$

Although the thermal conductivity has been assumed to be constant, it is in fact an implicit function of the radius since it varies with temperature and there is a radial distribution of the temperature.

This complication can be alleviated by assuming that the conductivity is constant within an annular region, with a value appropriate to the average temperature within that region. Then, by joining the solutions in adjacent regions, a temperature distribution can be obtained for the entire window. It is clear that as the number of regions within the window increases, the calculation becomes more realistic. Such a group of calculations is

shown in Fig. 9 for a one-, two-, and four-region approximation. In each of these cases the edge temperature is 80 K, 100 W is deposited in the central 2.5-cm diameter, and the disk thickness is 0.175 cm. As the figure shows, the temperature rise from the edge to the center is roughly 30–40 K. Higher power deposition will lead to higher temperature differentials. Consequently, this type of window does not look attractive at liquid nitrogen temperatures for higher heat deposition.

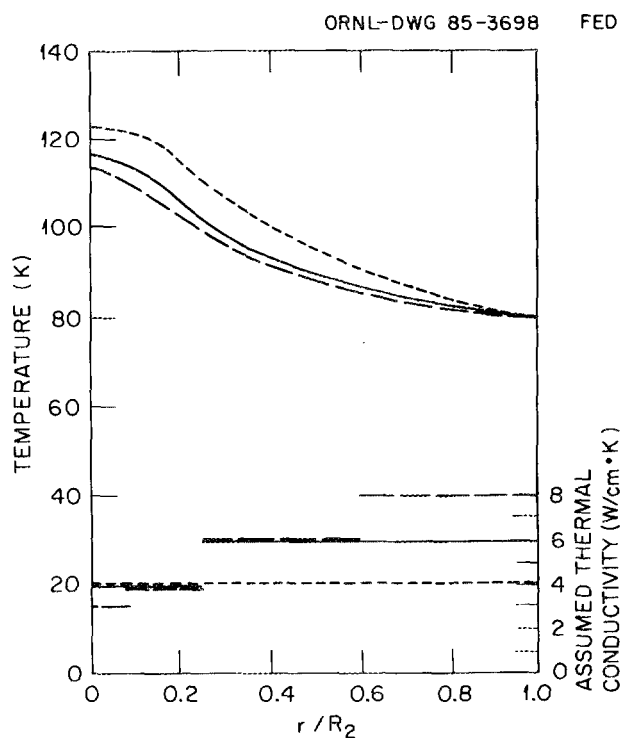
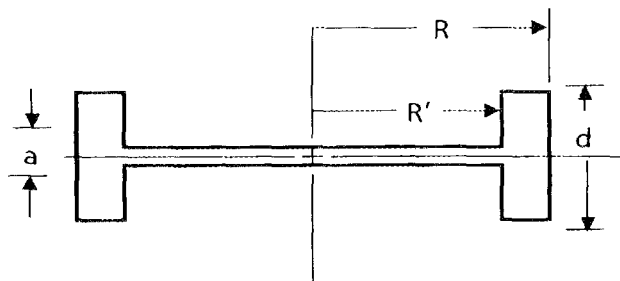


Fig. 9. Temperature distributions in an edge-cooled, single disk window. The thermal conductivity is assumed to have a constant value of 4 W/(cm·K) for the one-region model, and to change with radius as shown for the two- and four-region models.

By contrast, operation of an edge-cooled window at or below 20 K does appear attractive. The thermal conductivity can be 25 to 50 times greater, with the result that the power deposition could be higher by the same factor to give the same temperature increment. A window configured as shown in the next diagram would have an edge surface of $2\pi R d$ and a side surface of $2\pi(R^2 - R'^2)$.



For $R = 6.5$ cm, $R' = 5$ cm, and $d = 2.5$ cm, the total cooled surface area would be 200 cm². A heat transfer coefficient for gaseous helium of 0.174 W/(cm²·K) can be achieved with present-day technology and will result in a film drop of $P_T \div (0.174 \times 200) = 0.029P_T$. A four-region model was used with $R_1 = 0.1R$, $R_2 = 0.25R$, $R_3 = 0.5R$, and $a = 0.140$ cm. Equations (8) through (10) were used to determine $T_{(r=0)}$ for different powers absorbed between 10 and 500 W. The resulting central temperature used in Eq. (4) will conservatively calculate an absorptivity. Dividing Eq. (4) into the original assumed power absorbed will give the microwave throughput.

The results of the cases run are shown in Fig. 10. The figures show the gyrotron output power obtainable for a given power absorbed as a function of window coolant temperature. As can be seen, a 1-MW gyrotron window at 140 GHz appears quite feasible, and, depending on the ultimate accuracy of Eq. (4), a 10-MW window may be possible.

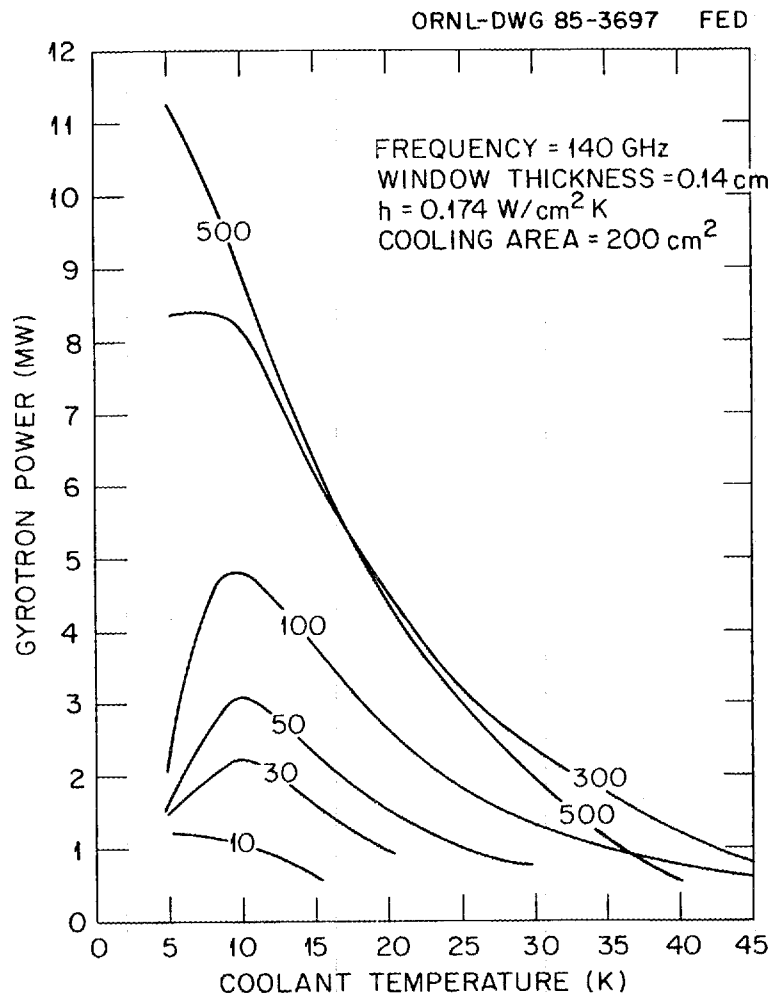


Fig. 10. Gyrotron output power vs coolant temperature for various values of the absorbed power in the window. A frequency of 140 GHz, a window thickness of 0.140 cm, a heat transfer coefficient of 0.174 W/(cm²·K), and a cooling area of 200 cm² were assumed.

4.4 OTHER HEAT LOADS

Operation of the window at cryogenic temperatures will result in additional heat loads due to conduction and radiation. These heat sources appear to be low enough to be tolerable. Another heat load not considered here is that due to natural convection. This would be a consideration if the waveguide beyond the window were filled with gas. In that case the gas would have to be kept dry to avoid ice condensation on the cold window. For the case of a vacuum waveguide, neither convection nor condensation would be a problem.

4.4.1 Conduction

Heat could be conducted to the window by several paths. A detailed analysis would have to await a more detailed window design. However, one seemingly unavoidable conduction path is that along the material that joins the window to the waveguide. This material is expected to be low-conductivity stainless steel, with a thin copper coating on the inside to minimize the microwave attenuation. If the stainless steel were 0.025 in. thick with a 2.5-in. diameter, then the cross-sectional area would be 1.27 cm^2 . If the length of the stainless steel section were 1 in., if the temperature difference were 200 K ($277 - 77$), and if the thermal conductivity were chosen¹⁰ to be $0.13 \text{ W}/(\text{cm}\cdot\text{K})$, then the power conducted to the window would be $\sim 13 \text{ W}$.

4.4.2 Radiation

An upper limit to the amount of power absorbed in the window can be obtained by assuming that (1) the window absorbs all the thermal radiation incident, (2) the emissivity of the waveguide and gyrotron materials is unity, (3) the solid angle subtended by the waveguide and gyrotron is 2π , and (4) the temperature of those materials is 400 K. In this case the radiant power absorbed is 2.3 W.

5. CONCLUSIONS

Reducing the operating temperature to cryogenic levels appears to be a very attractive way to increase the power handling capability of gyrotron windows. We have looked at both the single and double disk window designs operating between 5 and 80 K. The edge-cooled single disk window operating below $\sim 30 \text{ K}$ appears to be the simplest way of achieving $>1\text{-MW}$ cw output power at 140 GHz. In contrast to room temperature operation where thermal stress is the limiting mechanism, at cryogenic temperatures the normal runaway occurs when a relatively small change in temperature results in a large change in both thermal conductivity and dielectric loss tangent. Typically, the entire window temperature rises uniformly with power absorbed until the limit is reached.

The high thermal conductivity of sapphire offers an additional possibility in gyrotron window design. One of the most significant limitations thus far in high-average-power gyrotron tubes has been their narrow bandwidth. The narrow bandwidth is partly due to window designs that are compatible with cw operation. With a single disk sapphire window

operating below 30 K and grooved in the "night moth eye" configuration,¹¹ a broad bandwidth, high-average-power window would be possible. A gyroamplifier fitted with this type of window would offer great potential for fusion applications.

As a result of this study, two initial steps appear to be logical choices in the development of the cryogenic window. A conceptual design should be undertaken to more precisely determine heat loads, optimum operating temperatures, economics, etc. Also, a study of the dielectric properties of sapphire in the millimeter wave region as a function of temperature should be pursued.

REFERENCES

1. W. W. Ho, *Millimeter Wave Dielectric Property Measurement of Gyrotron Window Materials, Technical Report for the Period January 26, 1984*, SC 5357.4FR, Rockwell International Science Center, 1984.
2. M. K. Ferber, H. D. Kimrey, and P. F. Becher. "Mechanical Reliability of Ceramic Windows in High Frequency Microwave Heating Devices: Part I, An Analysis of Temperature and Stress Distribution," *J. Mater. Sci.* **19**, 3767-77 (1984).
3. W. B. Cook and S. Perkowitz, "Temperature Dependence of Ordinary Ray Far Infrared Optical Constants of Sapphire," conference proceedings.
4. E. V. Loewenstein, D. R. Smith, and R. L. Morgan, "Optical Constants of Far Infrared Materials, 2: Crystalline Solids," *Appl. Opt.* **12**(2), 398-406 (1983).
5. V. B. Braginsky and V. I. Panov, "Superconducting Resonators on Sapphire," *IEEE Trans. Magn.* **MAG-15**(1), 30-32 (1979).
6. Y. S. Touloukian and C. Y. Ho, eds., *Thermophysical Properties of Matter, vol. 2, Thermal Conductivity, Nonmetallic Solids*, IFI/Plenum, New York, 1970, pp. 12, 97; *vol. 1, Thermal Conductivity, Metallic Elements and Alloys*, IFI/Plenum, New York, 1970, p. 81.
7. D. E. Gray, ed., *American Institute of Physics Handbook*, 2d ed., McGraw-Hill, New York, 1963, p. 4-136.
8. D. H. Chung and G. Simmons, *J. Appl. Phys.* **39**, 5316 (1968).
9. P. F. Becher and M. K. Ferber, "Mechanical Reliability of Ceramic Windows in High Frequency Microwave Heating Devices: Part II, Mechanical Behavior of the Ceramics," *J. Mater. Sci.* **19**, 3778-85 (1984).
10. Y. S. Touloukian and C. Y. Ho, eds., *Thermophysical Properties of Matter, vol. 1, Thermal Conductivity, Metallic Elements and Alloys*, IFI/Plenum, New York, 1970, p. 1160.
11. J. Y. L. Ma and LA. C. Robinson, "Night Moth Eye Window for the Millimeter and Sub-millimeter Wave Region," *Opt. Acta* **130**(12), 1685-95 (1983).

INTERNAL DISTRIBUTION

- | | |
|---------------------|--|
| 1. F. W. Baity | 18. D. B. Thompson |
| 2. L. A. Berry | 19. T. L. White |
| 3. P. F. Becher | 20-21. Laboratory Records Department |
| 4. T. S. Bigelow | 22. Laboratory Records, ORNL-RC |
| 5. C. A. Foster | 23. Central Research Library |
| 6. H. H. Haselton | 24. Document Reference Section |
| 7-11. G. R. Haste | 25. Fusion Energy Division Library |
| 12. D. J. Hoffman | 26-27. Fusion Energy Division Publications
Office |
| 13-14. H. D. Kimrey | 28. ORNL Patent Office |
| 15. T. L. Owens | |
| 16-17. J. D. Prosis | |

EXTERNAL DISTRIBUTION

29. Office of the Assistant Manager for Energy Research and Development, U.S. Department of Energy, Oak Ridge Operations, Box E, Oak Ridge, TN 37831
30. F. Prevot, CEN/CADARACHE, Department de Recherches sur la Fusion Controllee, 13108 Saint-Paul-Lez-Durance, Cedex, France
31. J. D. Callen, Department of Nuclear Engineering, University of Wisconsin, Madison, WI 53706
32. J. F. Clarke, Associate Director for Fusion Energy, Office of Energy Research, ER-50 Germantown, U.S. Department of Energy, Washington, DC 20545
33. R. W. Conn, Department of Chemical, Nuclear, and Thermal Engineering, University of California, Los Angeles, CA 90024
34. S. O. Dean, Director, Fusion Energy Development, Science Applications International Corporation, 2 Professional Drive, Suite 249, Gaithersburg, MD 20879
35. H. K. Forsen, Bechtel Group, Inc., Research Engineering, P.O. Box 3965, San Francisco, CA 94105
36. T. V. George, Office of Fusion Energy, Office of Energy Research, Germantown ER531, U.S. Department of Energy, Washington, DC 20545
37. J. R. Gilleland, GA Technologies, Inc., Fusion and Advanced Technology, P.O. Box 81608, San Diego, CA 92138
38. R. W. Gould, Department of Applied Physics, California Institute of Technology, Pasadena, CA 91125
39. R. A. Gross, Plasma Research Laboratory, Columbia University, New York, NY 10027
40. D. M. Meade, Princeton Plasma Physics Laboratory, P.O. Box 451, Princeton, NJ 08544
41. M. Roberts, International Programs, Office of Fusion Energy, Office of Energy Research, ER-52 Germantown, U.S. Department of Energy, Washington, DC 20545
42. W. M. Stacey, School of Nuclear Engineering, Georgia Institute of Technology, Atlanta, GA 30332
43. D. Steiner, Rensselaer Polytechnic Institute, Nuclear Engineering Department, NES Building, Tibbets Avenue, Troy, NY 12181
44. R. Varma, Physical Research Laboratory, Navrangpura, Ahmedabad 380009, India

45. Bibliothek, Max-Planck Institut fur Plasmaphysik, D-8046 Garching, Federal Republic of Germany
46. Bibliothek, Institut fur Plasmaphysik, KFA, Postfach 1913, D-5170 Julich, Federal Republic of Germany
47. Bibliotheque, Centre de Recherches en Physique des Plasmas, 21 Avenue des Bains, 1007 Lausanne, Switzerland
48. Documentation S.I.G.N., Departement de la Physique du Plasma et de la Fusion Controlee, Centre d'Etudes Nucleaires, B.P. No. 85, Centre du Tri, 38041 Cedex, Grenoble, France
49. Library, Culham Laboratory, UKAEA, Abingdon, Oxfordshire, OX14 3DB, England
50. Library, FOM Institut voor Plasma-Fysica, Rijnhuizen, Jutphaas, The Netherlands
51. Library, Institute of Plasma Physics, Nagoya University, Nagoya 64, Japan
52. Library, International Centre for Theoretical Physics, Trieste, Italy
53. Library, Laboratorio Gas Ionizzati, Frascati, Italy
54. Library, Plasma Physics Laboratory, Kyoto University, Gokasho Uji, Kyoto, Japan
55. Plasma Research Laboratory, Australian National University, P.O. Box 4, Canberra, A.C.T. 2000, Australia
56. Thermonuclear Library, Japan Atomic Energy Research Institute, Tokai, Naka, Ibaraki, Japan
- 57-165. Given distribution as shown in TIC-4500 under Magnetic Fusion Energy (Category UC-20)